

# Exploration of the origin of large first hyperpolarizabilities of trisaza-bridged (36) fullerooids

Lizhi Jiang · Jingyang Gu · Xiaolei Zhu

Received: 11 November 2009 / Accepted: 25 January 2010 / Published online: 24 July 2010  
© Springer-Verlag 2010

**Abstract** We investigate theoretically the structures and second-order nonlinear optical (NLO) responses (first hyperpolarizabilities) of 15 trisaza-bridged (36) fullerooids (series-A) and 15 triborane-bridged (36) fullerooids (series-B). 3A has smaller transition energy and smaller ground state dipole moment, resulting in relatively larger static first hyperpolarizability (10647 au). Most trisaza-bridged (36) fullerooids have larger  $\beta$  values than the corresponding triborane-bridged (36) fullerooids. The  $f_0$  and  $\Delta\mu$  remain stable values when substituents R change for series-A except 2A and 5A (for series-B except 5B and 10B) and  $\beta$  values are proportional to  $\Delta E^3$ , which implies that the  $\beta$  values for series-A and series-B follow the two-level model. Results demonstrate that a proper bridge and lower transition energy  $\Delta E$  are more favorable to enlarging first hyperpolarizabilities of series-A and series-B. In addition, the frequency-dependent SHG and EOPE are also estimated and discussed. The current work can stimulate experimentalists to synthesize novel NLO materials designed in this work.

**Keywords** C<sub>36</sub> · Chromophore · First hyperpolarizability · Fullerene derivative · Non-linear optics

## Introduction

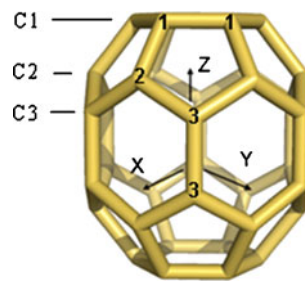
Fullerene derivatives with novel properties are of great potential application in material [1–3] and biomedical

sciences [4, 5]. Therefore, heterofullerenes [6–8], endohedral fullerene complexes with metals [9–11] and noble gases [12–14], and fullerene derivatives with chromophores [15, 16] have been widely synthesized. The three-dimensional conjugated  $\pi$  electron and the extensive charge delocalization [17] make fullerene derivatives exhibit high nonlinear optical (NLO) response. Fullerenes and their derivatives are also leading materials in photonic applications [18, 19]. The nonlinear optical properties including reverse saturation absorption, optical limiting [20–22], large third order nonlinear optical coefficient [23–25], and other nonlinear optical properties [26, 27] of fullerenes have been investigated. However, few fullerene derivatives with large first hyperpolarizabilities have been reported. In 2001, Barbosa [28] suggested a new approach for designing C<sub>36</sub> fullerene derivatives with large hyperpolarizabilities. Two types of trisaza-bridged (60) fullerenes were first synthesized by Tang et al. [29] and the optical limiting and large third-order nonlinear optical susceptibility were tested. On the other hand, a novel building block consisted of four trisaza-bridge (60) fullerooids was linked to a central cubane unit [30].

The smaller fullerene C<sub>36</sub> is much more reactive than C<sub>60</sub> and C<sub>70</sub> [28] and tends to form covalent bonds with other atoms or groups. The three kinds of carbon atoms for C<sub>36</sub> with D<sub>6h</sub> symmetry are marked as C1, C2, and C3, respectively as shown in Fig. 1. The (6, 5) open ring adducts are easy to be obtained in the addition reaction [29]. In the current work, we study the (6, 5) open ring adducts of C<sub>36</sub> as shown in Fig. 2, in which the trisaza-bridge and triborane-bridge moieties are bonded to the six-numbered ring on the top of C<sub>36</sub> cage. Interestingly, it is found that  $\beta$  values for series-A and series-B follow the two-level model. The current work provides primary physical insights into the origin of large first hyperpolarizabilities of the trisaza-

L. Jiang · J. Gu · X. Zhu (✉)  
State Key Laboratory of Materials-Oriented Chemical Engineering,  
College of Chemistry and Chemical Engineering,  
Nanjing University of Technology,  
Nanjing 210009, China  
e-mail: xlzhu@njut.edu.cn

**Fig. 1** Structure of C<sub>36</sub> with D<sub>6h</sub> symmetry. The three kinds of carbon atoms in C<sub>36</sub> are marked as C1, C2, and C3, respectively



bridged (36) fulleroids, which strongly suggests that some molecules designed in this work can be good candidates for synthesizing novel NLO materials.

## Calculation details

The energy of a system in an electric field can be represented as [31]

$$\mathbf{E} = \mathbf{E}^0 - \mu_i \mathbf{F}_i - \frac{1}{2} \alpha_{ij} \mathbf{F}_i \mathbf{F}_j - \frac{1}{6} \beta_{ijk} \mathbf{F}_i \mathbf{F}_j \mathbf{F}_k - \frac{1}{24} \gamma_{ijkl} \mathbf{F}_i \mathbf{F}_j \mathbf{F}_k \mathbf{F}_l + \dots \quad (1)$$

where E<sup>0</sup> is the energy of the system without electronic field and F<sub>i</sub> represents the components of the applied electronic field.  $\mu_i$ ,  $\alpha_{ij}$ ,  $\beta_{ijk}$ , and  $\gamma_{ijkl}$  are dipole moment, polarizability, the first and second hyperpolarizabilities, respectively. We use the HF/3-21G//CPHF/3-21G technique to investigate the structures, first hyperpolarizabilities, and other physical properties for designed systems, that is, the structures of the systems are optimized at the HF/3-21G level and vibrational frequency analysis is performed to examine the stabilities of the optimized geometries at the same level. The first hyperpolarizabilities and other physical properties are estimated at the CPHF/3-21G level. The static first hyperpolarizability is calculated in terms of

$$\beta_0 = (\beta_x^2 + \beta_y^2 + \beta_z^2)^{1/2}, \quad (2)$$

where

$$\beta_i = (3/5) \sum_{j=x,y,z} \beta_{ij}. \quad (3)$$

Two optical processes, namely, the second-harmonic generation (SHG) and electrooptical Pockels effect (EOPE) can be expressed as  $\beta(-2\omega; \omega, \omega)$  and  $\beta(-\omega; \omega, 0)$ , respectively. The frequency-dependent  $\beta$  can be denoted as [32]

$$\beta_{vec}(-2\omega; \omega, \omega) = \frac{1}{5} \sum_{\alpha=x,y,z} (\beta_{\xi\alpha\alpha} + 2\beta_{\alpha\xi\alpha}) \quad (4)$$

$$\beta_{vec}(-\omega; \omega, 0) = \frac{1}{5} \sum_{\alpha=x,y,z} (\beta_{\xi\alpha\alpha} + 2\beta_{\alpha\xi\alpha}) \quad (5)$$

where  $\xi$  is the molecular-fixed dipole moment axis. The frequency-dependent first hyperpolarizabilities ( $\beta(-2\omega; \omega, \omega)$  and  $\beta(-\omega; \omega, 0)$ ) of trisaza-bridged (36) fulleroids are also calculated at the CPHF/3-21G level. All calculations are performed using GAUSSIAN 09 program package [33].

## Results and discussion

### Equilibrium structure

30 optimized structures of trisaza-bridged (36) fulleroids and triborane-bridged (36) fulleroids are obtained. It is well known that the first hyperpolarizabilities ( $\beta$ ) are very sensitive to the geometry structures [34, 35]. As shown in Fig. 1, the calculated C1-C1, C1-C2, C2-C3, and C3-C3 bond distances of C<sub>36</sub> are 1.42, 1.50, 1.44, and 1.45 Å, respectively. It is noted that after trisaza-bridge is attached to C<sub>36</sub>, the C<sub>36</sub> part exhibits significant geometrical change.

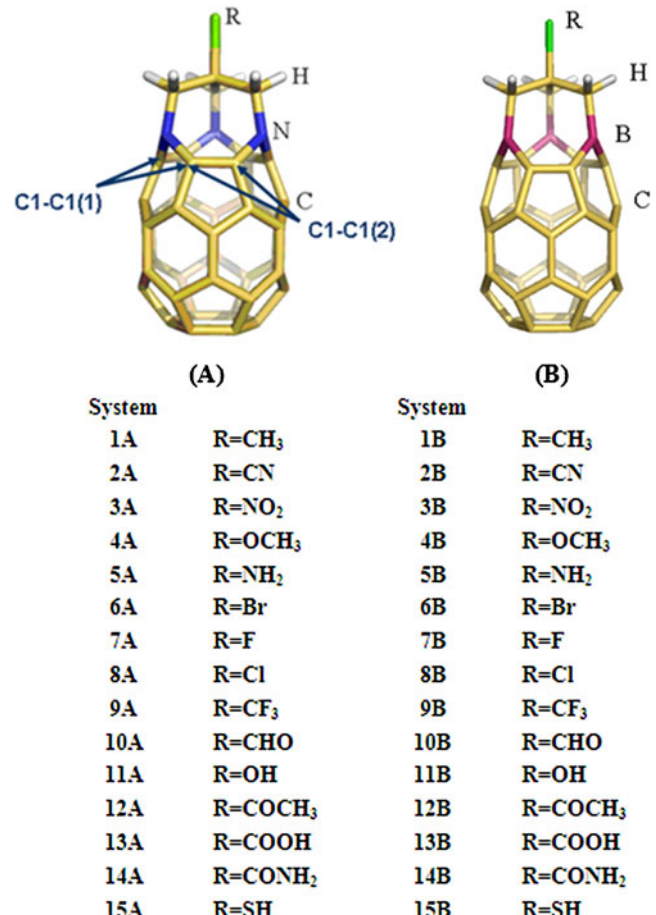


**Fig. 2** Optimized structures of trisaza-bridged (36) fulleroids (series-A) and triborane-bridged (36) fulleroids (series-B)

**Table 1** The physical properties of trisaza-bridged (36)fulleroids

System	R	Point group	$\alpha^a$ (au)	$\beta$ (au)	Ratio <sup>b</sup>	$\mu^a$ (D)	$\Delta\mu^a$ (D)	$\Delta E^a$ (eV)	$f_0^a$
1A	CH <sub>3</sub>	C <sub>3V</sub>	331.62	5740	3.99	15.81	7.26	0.7902	0.0045
2A	CN	C <sub>3V</sub>	341.22	2592	2.17	5.55	4.37	1.3678	0.0012
3A	NO <sub>2</sub>	C <sub>1</sub>	339.83	10647	6.67	9.75	6.91	0.6402	0.0059
4A	OCH <sub>3</sub>	C <sub>1</sub>	335.95	6319	4.31	15.28	7.17	0.7632	0.0049
5A	NH <sub>2</sub>	C <sub>1</sub>	336.19	2777	2.33	1.10	5.14	1.3000	0.0014
6A	Br	C <sub>3</sub>	343.07	8309	5.54	12.63	7.22	0.7064	0.0053
7A	F	C <sub>3V</sub>	322.96	7684	5.05	12.48	7.06	0.7063	0.0052
8A	Cl	C <sub>3V</sub>	339.97	9050	5.86	11.50	7.13	0.6826	0.0054
9A	CF <sub>3</sub>	C <sub>3V</sub>	331.19	8240	5.43	11.91	7.03	0.6925	0.0054
10A	CHO	C <sub>1</sub>	333.75	7245	4.87	13.11	7.00	0.7282	0.0052
11A	OH	C <sub>S</sub>	324.90	6550	4.42	14.31	7.07	0.7481	0.0049
12A	COCH <sub>3</sub>	C <sub>1</sub>	343.18	6920	4.75	14.16	7.02	0.7433	0.0049
13A	COOH	C <sub>1</sub>	335.06	6874	4.71	14.60	7.12	0.7425	0.0050
14A	CONH <sub>2</sub>	C <sub>1</sub>	337.75	6851	4.73	14.39	6.83	0.7420	0.0050
15A	SH	C <sub>S</sub>	343.59	7661	5.14	13.24	7.20	0.7251	0.0053

<sup>a</sup>  $\alpha$  represents polarizability,  $\mu$  is dipole moment,  $\Delta\mu = |\mu_g - \mu_e|$ ,  $\Delta E$  accounts for transition energy, and  $f_0$  is oscillator strength

<sup>b</sup> The “Ratio” accounts for the ratio of the maximal main diagonal element of  $\beta$  tensor

( $\beta_{MDE}^{\max}$ ) and maximal non-main diagonal element of  $\beta$  tensor ( $\beta_{NMDE}^{\max}$ )

As shown in Table 1, 1A, 3A, 4A, and 6A-15A have relatively large  $\beta$  value. The averaged C1-C1(1) distance (in the (6, 5) open ring) and C1-C1(2) distance (in the (6, 5) closed ring) are about 2.207 Å and 1.324 Å, respectively, and the averaged C1-C2 and C2-C3 bond distances are 1.502 and 1.420 Å, respectively. However, 2A and 5A exhibit relatively smaller  $\beta$  values and the averaged C1-C1(1) and C1-C1(2) distances are about 2.260 and 1.350 Å, respectively. As mentioned by Tang [29], attaching trisaza-bridge moiety to C<sub>36</sub> leads to a hole on the fullerene surface. The relevant bond lengths as mentioned above reveal that 2A and 5A have larger holes on the surfaces of C<sub>36</sub> than other series-A molecules.

It is well known that the UV/Vis spectra [36, 37] are a useful tool for distinguishing the structures. The UV-vis spectra are calculated at the CIS/3-21G level, and 50 excited states are selected. For comparison, six series-A molecules (1A ( $\beta=5740$  au), 3A ( $\beta=10647$  au), 8A ( $\beta=9050$  au), 9A ( $\beta=8240$  au), 2A ( $\beta=2592$  au), 5A ( $\beta=2777$  au)), and six series-B molecules (1B ( $\beta=3750$  au), 3B ( $\beta=4884$  au), 8B ( $\beta=4652$  au), 9B ( $\beta=4374$  au), 2B ( $\beta=2639$  au), 5B ( $\beta=3078$  au)) are examined. Their UV/Vis spectra are displayed in Fig. 3. We take series-A as an example. It is worth to mention that 1A, 3A, 8A, and 9A exhibit similar absorption peaks in the UV/Vis spectra, while 2A and 5A also have similar ones. Obviously, C<sub>36</sub> part has conjugated character. As shown in Fig. 3, the first adsorption peak is attributed to the  $\pi-\pi^*$  transition of C<sub>36</sub> itself. 2A and 5A with larger C1-C1(1) and C1-C1(2) distances have larger holes on the surfaces of C<sub>36</sub>, caused by trisaza-bridges, than other systems as mentioned above. In fact, the C<sub>36</sub> part (except the top layer) of 2A and 5A exhibit more delocalized structure, which results in red shift of the first adsorption peak compared to the corresponding peaks of other series-A molecules as shown in Fig. 3(a). The second peaks (370~400 nm) of 2A and 5A correspond to

9050au), 9A ( $\beta=8240$  au), 2A ( $\beta=2592$  au), 5A ( $\beta=2777$  au)), and six series-B molecules (1B ( $\beta=3750$  au), 3B ( $\beta=4884$  au), 8B ( $\beta=4652$  au), 9B ( $\beta=4374$  au), 2B ( $\beta=2639$  au), 5B ( $\beta=3078$  au)) are examined. Their UV/Vis spectra are displayed in Fig. 3. We take series-A as an example. It is worth to mention that 1A, 3A, 8A, and 9A exhibit similar absorption peaks in the UV/Vis spectra, while 2A and 5A also have similar ones. Obviously, C<sub>36</sub> part has conjugated character. As shown in Fig. 3, the first adsorption peak is attributed to the  $\pi-\pi^*$  transition of C<sub>36</sub> itself. 2A and 5A with larger C1-C1(1) and C1-C1(2) distances have larger holes on the surfaces of C<sub>36</sub>, caused by trisaza-bridges, than other systems as mentioned above. In fact, the C<sub>36</sub> part (except the top layer) of 2A and 5A exhibit more delocalized structure, which results in red shift of the first adsorption peak compared to the corresponding peaks of other series-A molecules as shown in Fig. 3(a). The second peaks (370~400 nm) of 2A and 5A correspond to

**Fig. 3** UV/Vis spectra of six molecules of series-A (a) and six molecules of series-B(b)

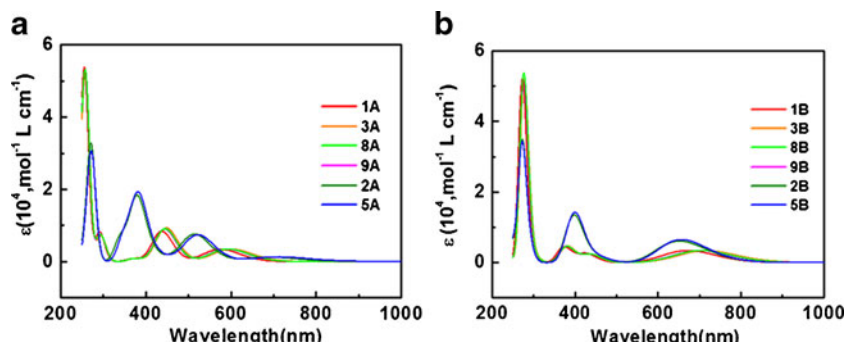
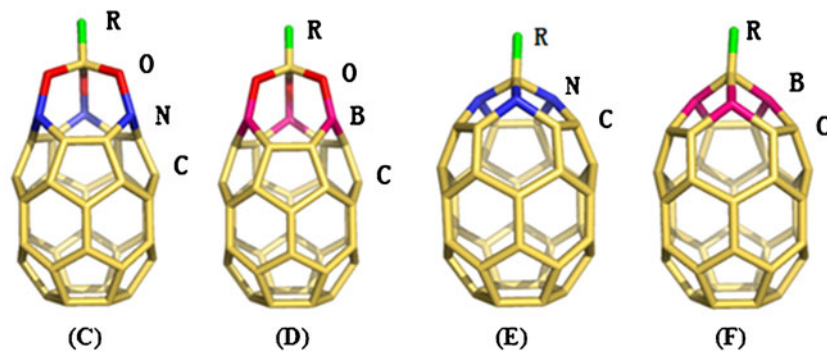


**Fig. 4** Optimized structures of the molecules for series-C~series-F



System	System	System	System
3C      R=NO <sub>2</sub>	3D      R=NO <sub>2</sub>	3E      R=NO <sub>2</sub>	3F      R=NO <sub>2</sub>
8C      R=Cl	8D      R=Cl	8E      R=Cl	8F      R=Cl
9C      R=CF <sub>3</sub>	9D      R=CF <sub>3</sub>	9E      R=CF <sub>3</sub>	9F      R=CF <sub>3</sub>
11C     R=OH	11D     R=OH	11E     R=OH	11F     R=OH
2C      R=CN	2D      R=CN	2E      R=CN	2F      R=CN
5C      R=NH <sub>2</sub>	5D      R=NH <sub>2</sub>	5E      R=NH <sub>2</sub>	5F      R=NH <sub>2</sub>
	1D      R=CH <sub>3</sub>		
	7D      R=F		
	13D     R=COOH		
	15D     R=SH		

photoinduced ligand-to-fullerene charge transfer process with  $\sigma \rightarrow \pi^*$  character. For other series-A molecules, this peak shows red-shift (400~500 nm). In addition, the other bands in visible region are caused by  $n \rightarrow \pi^*$  transitions, which are related to substitutes (R).

#### The static first hyperpolarizabilities

Some physical parameters of the trisaza-bridged (36) fulleroids are summarized in Table 1. It is well known that the first hyperpolarizability of C<sub>36</sub> with D<sub>6h</sub> symmetry is 0. Upon attaching trisaza-bridge moiety to C<sub>36</sub>, the symmetries of the derived trisaza-bridge (36) fulleroids decrease and their first hyperpolarizabilities significantly increase, which suggests that the trisaza-bridge moiety may play an important role in enlarging first hyperpolarizability. In order to support the above conclusion, the trisaza-bridge moiety (-C(CH<sub>2</sub>N)<sub>3</sub>) of 8A is removed, resulting in  $\beta$  value of 861 au, which is only one-tenth of that (9050 au) of 8A as shown in Table 1.

In order to further explore the contribution of the trisaza-bridge (-C(CH<sub>2</sub>N)<sub>3</sub>) (or triborane-bridge (-C(CH<sub>2</sub>B)<sub>3</sub>) to  $\beta$  values, we design four series molecules (series-C~series-F). Series-C and series-D can be derived by replacing each -CH<sub>2</sub>- group in the bridges of series-A and series-B using oxygen atom while series-E and series-F can be obtained by removing three -CH<sub>2</sub>- groups in the bridges of series-A and series-B as shown in Fig. 4. The optimized structures for series-C~series-F are obtained at the HF/3-21G level, the first hyperpolarizabilities and some physical properties are

computed at the CPHF/3-21G level and listed in Table 2. It is noted that for series-C~series-F, their  $\beta$  values are relatively smaller. Moreover, their  $\beta$  values are not sensitive to different substituents (R) except series-D. It is clear that for series-E and series-F, the shorter bridge results in significant decrease of  $\beta$  values. It demonstrates that the trisaza-bridge (or triborane-bridge) moiety plays an important role in enlarging first hyperpolarizability.

In order to examine the role of the three N atoms in the trisaza-bridge moiety in enlarging  $\beta$ , the three N atoms in the bridge are replaced by three B atoms, resulting in 15 structures of triborane-bridged (36) fulleroids. The opti-

**Table 2** The first hyperpolarizabilities and dipole moment for series-C~series-F

System	$\beta$ (au)	$\mu$ (D)	System	$\beta$ (au)	$\mu$ (D)
3C	2276	12.21	3E	2051	8.41
8C	2312	14.52	8E	2061	10.64
9C	2338	11.49	9E	2136	7.77
11C	2356	9.43	11E	2108	5.22
2C	2345	12.91	2E	2123	9.43
5C	2520	12.60	5E	2220	3.05
3D	7796	5.72	3F	1730	9.74
8D	1980	13.89	8F	1594	11.94
9D	7707	6.39	9F	1814	9.30
11D	6043	9.03	11F	1900	6.82
2D	2063	12.22	2F	1603	11.61
5D	2406	6.05	5F	1964	5.60

**Table 3** The physical properties of triborane-bridged (36) fulleroids

System	R	Point group	$\alpha^a$ (au)	$\beta$ (au)	Ratio <sup>b</sup>	$\mu^a$ (D)	$\Delta\mu^a$ (D)	$\Delta E^a$ (eV)	$f_0^a$
1B	CH <sub>3</sub>	C <sub>3V</sub>	346.56	3750	1.95	14.27	7.63	1.0315	0.0028
2B	CN	C <sub>3V</sub>	357.33	2639	1.94	8.62	7.16	1.1266	0.0020
3B	NO <sub>2</sub>	C <sub>1</sub>	350.63	4884	2.43	8.07	7.48	0.9024	0.0034
4B	OCH <sub>3</sub>	C <sub>1</sub>	351.25	3888	1.97	13.64	7.56	1.0076	0.0029
5B	NH <sub>2</sub>	C <sub>1</sub>	352.76	3078	2.30	3.54	0.28	1.0558	0.0023
6B	Br	C <sub>1</sub>	355.67	4467	2.28	10.73	7.68	0.9550	0.0032
7B	F	C <sub>3V</sub>	336.46	4212	2.11	10.97	7.51	0.9601	0.0031
8B	Cl	C <sub>3V</sub>	352.14	4652	2.32	9.57	7.62	0.9322	0.0033
9B	CF <sub>3</sub>	C <sub>3V</sub>	343.92	4374	2.22	10.35	7.54	0.9481	0.0031
10B	CHO	C <sub>1</sub>	355.80	2777	2.01	6.32	4.36	1.0922	0.0022
11B	OH	C <sub>1</sub>	339.56	3912	1.98	12.79	7.46	0.9962	0.0029
12B	COCH <sub>3</sub>	C <sub>1</sub>	357.51	4097	2.14	12.49	7.33	0.9899	0.0030
13B	COOH	C <sub>1</sub>	349.07	4097	2.13	12.97	7.51	0.9920	0.0030
14B	CONH <sub>2</sub>	C <sub>1</sub>	351.86	4050	2.13	12.75	7.05	0.9892	0.0030
15B	SH	C <sub>S</sub>	356.84	4328	2.21	11.47	7.59	0.9708	0.0031

<sup>a</sup>  $\alpha$  represents polarizability,  $\mu$  is dipole moment,  $\Delta\mu = |\mu_g - \mu_e|$ ,  $\Delta E$  accounts for transition energy, and  $f_0$  is oscillator strength

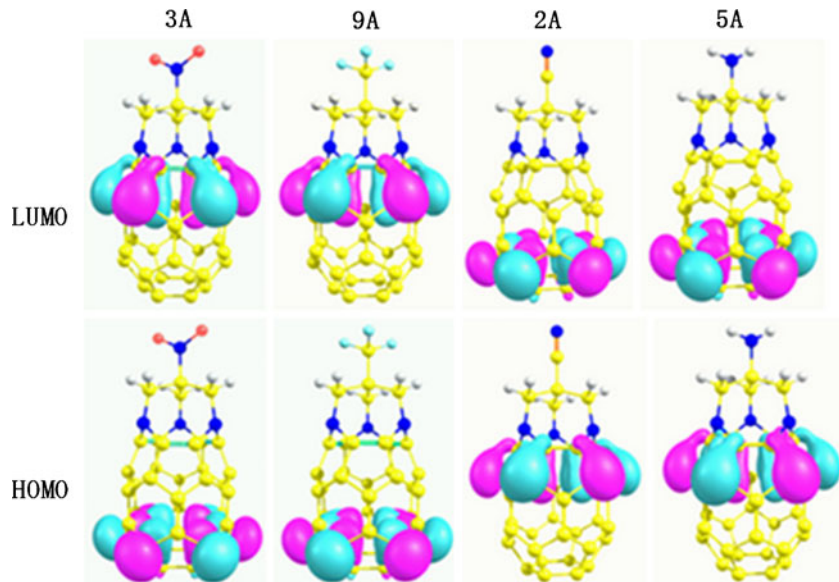
<sup>b</sup> The “Ratio” accounts for the ratio of the maximal main diagonal element of  $\beta$  tensor ( $\beta_{MDE}^{\max}$ ) and maximal non-main diagonal element of  $\beta$  tensor ( $\beta_{NMDE}^{\max}$ )

mized structures of triborane-bridged (36) fulleroids and physical properties are represented in Fig. 2 and Table 3. Clearly, their  $\beta$  values are smaller than corresponding values of trisaza-bridged (36) fulleroids, which reveals that electron-rich nitrogen atoms are more favorable to increasing  $\beta$  compared to the electron-deficient boron atoms

It is found that most structures of series-A have similar HOMO and LUMO orbitals like 3A and 9A while 2A and 5A show reverse results as shown in Fig. 5. For series-B molecules, similar phenomenon is also observed, that is, the

HOMO and LUMO orbitals of series-B molecules are similar to 3A except 2B, 5B, and 10B. The charge distribution of the ground state is often indicative of the nature of the molecular moieties. Therefore, first, we examine the charge distribution of the ground state for trisaza-bridge fulleroids. It is found that the positive charges (1.79 and 1.73e) on fullerene moieties of 2A and 5A are more than those (1.57~1.66e) of other molecules of series-A, which clearly suggests that C<sub>36</sub> in series-A is electron donor. Substituents (R) have positive or negative charges,

**Fig. 5** HOMO and LUMO orbitals for the trisaza-bridged (36) fulleroids with R=NO<sub>2</sub> (3A), CF<sub>3</sub> (9A), CN (2A), and NH<sub>2</sub> (5A)



which is mainly caused by the complicated  $-(\text{NCH}_2)_3-$  bridge in series-A. In order to explain the results of Fig. 5, we further examine the charge transfer between ground state and first excited state for each atom. Mulliken charge analysis demonstrates that the charge of  $\sim 0.07e$  transfers from  $\text{C}_{36}$  moiety to the trisaza-bridged part and substituent (R) for each of series-A except 2A and 5A, which is consistent with the results from Fig. 5. In the case of series-B, the charge of  $\sim 0.1e$  transfers from  $\text{C}_{36}$  moiety to the triborane-bridged part and substituent R except 2B, 5B and 10B. It suggests that  $\text{C}_{36}$  moiety is a good donor and the charge transfer between  $\text{C}_{36}$  and trisaza-bridge (or triborane-bridge) part as well as substituent (R) has influence on first hyperpolarizability.

In order to further investigate the origin of larger  $\beta$  values of series-A and series-B, we use the following two-level model to examine the main influencing factors of  $\beta$  [38, 39],

$$\beta_0 = (3/2) \Delta\mu f_0 / \Delta E^3 \quad (6)$$

where  $\Delta E$ ,  $f_0$ , and  $\Delta\mu$  are the transition energy, oscillator strength, and the difference in dipole moment between the ground state and the first excited state, respectively. For series-A and series-B,  $\Delta E$ ,  $f_0$ , and  $\Delta\mu$  are estimated at the CIS/3-21G level and listed in Tables 1 and 3, respectively. It is interesting to note that from Tables 1 and 3 that  $f_0$  and  $\Delta\mu$  do not appear to significantly change when substitutes (R) change for the molecules of series-A except 2A and 5A (for series-B except 5B and 10B). If we plot  $\beta$  against  $\Delta E^{-3}$  for series-A and series-B, an approximately linear relation is observed as shown in Fig. 6(a), that is,  $\beta$  values are proportional to  $\Delta E^{-3}$ , which reveals that the  $\beta$  values for series-A and series-B follow the two-level model and transition energy  $\Delta E$  is one controlling factor for  $\beta$ . Since  $f_0 = \Delta\mu^2 \Delta E$ , in that case, an equation analogous to Eq. 6 demonstrates that the first hyperpolarizability is proportional to  $\Delta E^{-2}$ , which is supported by Fig. 6(b).

It is not difficult to note from Tables 1 and 3 that the dipole moments of trisaza-bridged (or triborane-bridged) (36)

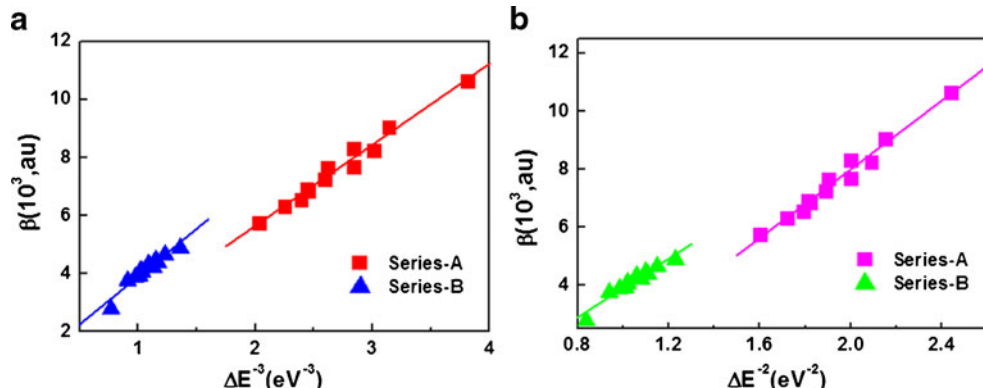
fulleroids are relatively larger because of the large charge separation between the  $\text{C}_{36}$  moiety and the trisaza-bridge (or triborane-bridge) moiety. It is well known that strong dipole-dipole interactions in a system with large dipole moment will lead to a centrosymmetric crystal [40], which may make the second-order NLO response vanish. Fortunately, their  $\beta$  values are inversely proportional to ground state dipole moment as shown in Fig. 7. Generally, for conventional D- $\pi$ -A systems [39–42], large ground state dipoles are favorable to increasing  $\beta$  values. However, for the molecules designed in current work, 3A with larger  $\beta$  value (10647au) has relatively smaller dipole moment (9.75D). These structures are different from the traditional D- $\pi$ -A systems. The relationship between the  $\beta$  and the ground state dipole moment demonstrates that the reduction of the ground state dipole moment is favorable to increasing  $\beta$  value.

The “ratio” in Tables 1 and 3 accounts for the ratio of the maximal main diagonal element of  $\beta$  tensor ( $\beta_{\text{MDE}}^{\max}$ ) and maximal non-main diagonal element of  $\beta$  tensor ( $\beta_{\text{NMDE}}^{\max}$ ). The data in Tables 1 and 3 show that the ratios of  $\beta_{\text{MDE}}^{\max} / \beta_{\text{NMDE}}^{\max}$  are about 1.9~6.7. Figure 8 represents the correlation of  $\beta$  with  $\beta_{\text{MDE}}^{\max} / \beta_{\text{NMDE}}^{\max}$ . It reveals that the  $\beta_{\text{MDE}}^{\max}$  have larger contribution to the  $\beta$  value and the designed systems in this work are one-dimensional charge transfer systems.

#### Frequency-dependent first hyperpolarizability

The averaged values of the  $\beta(-2\omega; \omega, \omega)$  and  $\beta(-\omega; \omega, 0)$  in the region of applied frequencies are computed in terms of Eqs. 4 and 5 as mentioned above. Since 3A, 8A and 9A have relatively larger static first hyperpolarizabilities, we examine frequency-dependent first hyperpolarizabilities ( $\beta(-2\omega; \omega, \omega)$  and  $\beta(-\omega; \omega, 0)$ ) for them as shown in Figs. 9 and 10. As shown in Fig. 9(a), for 9A, the dispersion of the  $\beta(-2\omega; \omega, \omega)$  is positive up to  $2\omega = 0.045$  a.u. Then, it tends to be strongly negative in the region  $2\omega = [0.045, 0.050]$  a.u., which encompasses the transition frequency  $\omega_{\text{CT}}$  of the charge transfer state. In addition, as shown in Fig. 9(b), for 8A, it is interesting to

**Fig. 6** Relationship between  $\beta$  and transition energy for series-A and series-B. (a) for  $\beta \sim \Delta E^{-3}$ ; (b) for  $\beta \sim \Delta E^{-2}$



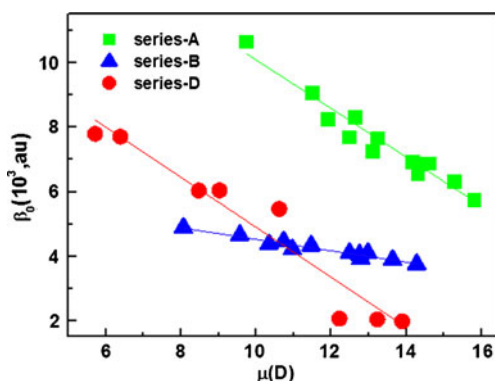


**Fig. 7** Correlation of  $\beta$  values with dipole moments for series-A, series-B, and series-D

note that there is a platform between two peaks of  $\beta(-2\omega; \omega, \omega)$ . The dispersion of  $\beta(-2\omega; \omega, \omega)$  for 3A exhibits reverse trend, which may be attributed to the negative dipole moment along the x axis. It is not difficult to see from Fig. 10 that there is a positive peak near  $\omega=0.025$  au for 8A and a negative peak near  $\omega=0.0225$  au for 3A, which may also be associated with the direction of the dipole moment. For 9A, the peak of  $\beta(-\omega; \omega, 0)$  is relatively smaller. However, for 8A and 3A, there are very strong peaks near resonance frequency. The SHG and EOPE at different frequency  $\omega$  showed in Figs. 9 and 10 indicate that if the larger frequency does not adopt, the stronger resonance will be induced, which is consistent with the recent reports [43, 44].

## Conclusions

The structures and first hyperpolarizabilities of 15 trisaza-bridged (36) fulleroles (series-A) and 15 triborane-bridged (36) fulleroles (series-B) are systematically investigated. The main contributions are as follows: (i) the combination

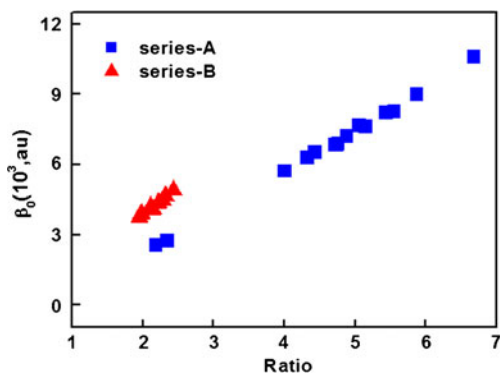


**Fig. 8** Correlation of  $\beta$  values with ratio for series-A and series-B. The “ratio” accounts for the ratio of the maximal main diagonal element of  $\beta$  tensor ( $\beta_{MDE}^{\max}$ ) with maximal non-main diagonal element of  $\beta$  tensor ( $\beta_{NMDE}^{\max}$ )

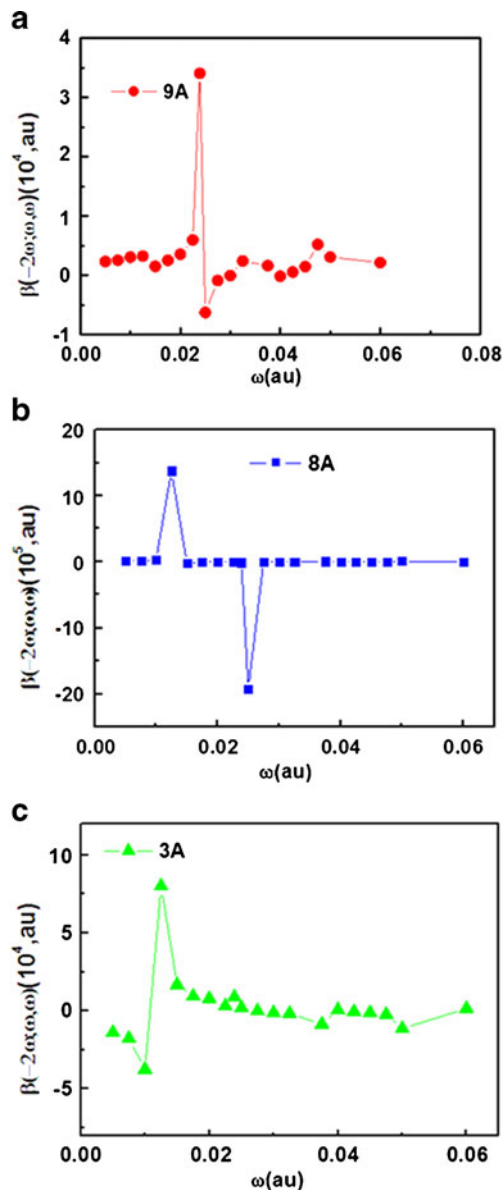


**Fig. 9** The relationship of the averaged first-order hyperpolarizability  $\beta(-2\omega; \omega, \omega)$  and the applied frequency

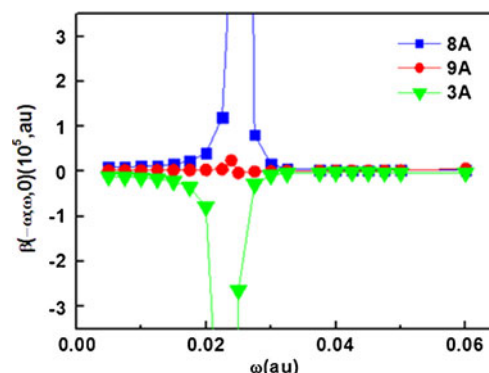


**Fig. 10** The relationship of the averaged first-order hyperpolarizability  $\beta(-\omega; \omega, 0)$  and the applied frequency\*

of C<sub>36</sub>, trisaza-bridge(C(CH<sub>2</sub>N)<sub>3</sub>)), and -NO<sub>2</sub> substitute (for 3A) leads to relatively larger static first hyperpolarizability (10647 au). It is due to the fact that 3A has smaller transition energy and smaller ground state dipole moment. 3A may be a good candidate for high-performance NLO material; (ii) most trisaza-bridged (36) fulleroids have larger  $\beta_0$  values than the corresponding triborane-bridged (36) fluoroiods. Thus, choosing a proper bridge is an important factor in the search for fullerene derivatives with large NLO responses; (iii) the f<sub>0</sub> and Δu keep stable values when substitutes (R) change for series-A except 2A and 5A (for series-B except 5B and 10B) and β values are proportional to ΔE<sup>3</sup>, which reveals that the β values for series-A and series-B satisfy the two-level model and transition energy ΔE plays the crucial role in enlarging first hyperpolarizability of series-A and series-B; (iv) the frequency-dependent SHG and EOPE reveal that if the larger frequency does not adopt, the stronger resonance will be induced, which is consistent with the observations by Kanatzidis et al. Moreover, when we screen high-performance NLO materials, we should consider not only the static β but also the frequency-dependent β. The current work will be valuable for experimentalists to design high-performance NLO materials.

**Acknowledgments** This work is supported by grants from the National Science Foundation of China (No. 20706029, 20876073), Jiangsu Science and Technology Department of China (No. BK2008372), and Nanjing University of Technology of China (No. ZK200803). We want to express our thanks for Reviewers' valuable suggestions for this article.

## References

- Innocenzi P, Brusatin G (2001) Fullerene-based organic-inorganic nanocomposites and their applications. *Chem Mater* 13:3126–3139
- D'Souza F, Chitta R, Sandanayaka ASD, Subbaiyan NK, D'Souza L, Araki Y, Ito O (2007) Supramolecular carbon nanotube-fullerene Donor-acceptor hybrids for photoinduced electron transfer. *J Am Chem Soc* 129:15865–15871
- Pupyshova OV, Farajian AA, Yakobson BI (2008) Fullerene nanocage capacity for hydrogen storage. *Nano Lett* 8:767–774
- Nielsen GD, Roursgaard M, Jensen AK, Poulsen SS, Larsen ST (2008) In vivo biology and toxicology of fullerenes and their derivatives. *Basic Clin Pharmacol & Toxicol* 103:197–208
- Markovic Z, Trajkovic V (2008) Biomedical potential of the reactive oxygen species generation and quenching by fullerenes (C<sub>60</sub>). *Biomaterials* 29:3561–3573
- Gu FL, Chen Z, Jiao H, Tian WQ, Aoki Y, Thiel W, Ragué Schleyer P (2004) Study on the optical and magnetic properties of C<sub>48</sub>N<sub>12</sub> azafullerene isomers. *Phys Chem Chem Phys* 6:4566–4570
- Cheng WD, Wu DS, Zhang H, Chen DG, Wang HX (2002) Optimizat-ion of geometrical structure and simulation of the spectra of third-order nonlinear optical polarizabilities in C<sub>59</sub>Si and C<sub>58</sub>Si<sub>2</sub> heterofullerenes. *Phys Rev B* 66:085422/1–085422/10
- Emanuele E, Negri F, Orlandi G (2007) Structure, stability and spect-roscopic properties of isomers of C<sub>48</sub>B<sub>6</sub>N<sub>6</sub> heterofullerene with isolated and sequential BN substitutional patterns. *Inorg Chim Acta* 360:1052–1062
- Pavanello M, Jalbout AF, Trzaskowski B, Adamowicz L (2007) Full- erene as an electron buffer: Charge transfer in Li@C<sub>60</sub>. *Chem Phys Lett* 442:339–343
- Stevenson S, Thompson MC, Coumbe HL, Mackey MA, Umbe CE, PaigeJ PJ (2007) Chemically adjusting plasma temperature, energy, and reactivity (CAPTEAR) method using NO<sub>x</sub> and combustion for selectivesynthesis of Sc<sub>3</sub>N@C<sub>80</sub> metallic nitride fullerenes. *J Am Chem Soc* 129:16257–16262
- Osuna S, Swart M, Campanera JM, Poblet JM, Solà M (2008) Chemical reactivity of D<sub>3h</sub> C<sub>78</sub> (Metallo)fullerene: regioselectivity changes induced by Sc<sub>3</sub>N encapsulation. *J Am Chem Soc* 130:6206–6214
- Shabtai E, Weitz A, Haddon RC, Hoffman RE, Rabinovitz M, Khong A, Cross RJ, Saunders M, Cheng PC, Scott LT (1998) <sup>3</sup>He NMR of He@C<sub>60</sub><sup>6-</sup> and He@C<sub>70</sub><sup>6-</sup>. new records for the most shielded and the most deshielded <sup>3</sup>He inside a fullerene<sup>1</sup>. *J Am Chem Soc* 120:6389–6393
- Ross MM, Callahan JH (1991) Formation and characterization of carbon mol.-helium (C<sub>60</sub>He<sup>+</sup>). *J Phys Chem* 95:5720–5723
- Saunders M, Cross RJ, Jimenez-Vazquez HA, Shimshi R, Khong A (1996) Noble gas atoms inside fullerenes. *Science* 271:1693–1697
- Xiao Z, Yao J, Yang D, Wang F, Huang S, Gan L, Jia Z, Jiang Z, Yang X, Zheng B, Yuan G, Zhang S, Wang Z (2007) Synthesis of (59) fullerenones through peroxide-mediated stepwise cleavage of fullerene skeleton bonds and X-ray structures of their water-encapsulated open-cage complexes. *J Am Chem Soc* 129:16149–16162
- Zhang WB, Tu Y, Ranjan R, Van Horn RM, Leng S, Wang J, Polce MJ, Wesdemiotis C, Quirk RP, Newkome GR, Cheng SZD (2008) “Clicking” fullerene with polymers: Synthesis of (60) fullerene end-capped polystyrene. *Macromolecules* 41:515–517
- Guldi DM (2000) Fullerenes: Three dimensional electron acceptor materials. *Chem Commun* 321–327
- Singh CP, Roy S (2004) Dynamics of all-optical switching in C<sub>60</sub> and its application to optical logic gates. *Opt Eng* 43:426–431
- Cui YH, Chen DL, Tian WQ, Feng JK (2007) Structures, stabilities, and electronic and optical properties of C<sub>62</sub> fullerene isomers. *J Phys Chem A* 111:7933–7939
- Elima HI, Ouyang J, Goh SH, Jia W (2005) Optical-limiting-based materials of mono-functional, multi-functional and supramolecular C<sub>60</sub>-containing polymers. *Thin Solid Films* 477:63–72
- Allaf AW, Zidamb MD (2005) Optical limiting behavior of new fullerene derivatives. *Opt Lasers Eng* 43:57–62
- Tong R, Wu H, Li B, Zhu R, You G, Qian S, Lin Y, Cai R (2005) Reverse saturable absorption and optical limiting performance of fullerene-functionalized polycarbonates in femtosecond time scale. *Physica B* 366:192–199
- Mateo-Alonso A, Iliopoulos K, Couris S, Prato M (2008) Efficient modulation of the third order nonlinear optical properties of fullerene derivatives. *J Am Chem Soc* 130:1534–1535
- Jensen L, Astrand PO, Mikkelsen KV (2004) The static polarizability and second hyperpolarizability of fullerenes and carbon nanotubes. *J Phys Chem A* 108:8795–8800
- Li K, Chen Q, Sargent EH, Wang ZY (2003) (60) Fullerene-containing polyurethane films with large ultrafast nonresonant third-order nonlinearity at telecommunication wavelengths. *J Am Chem Soc* 125:13648–13649
- Elim HI, Anandakathir R, Jakubiak R, Chiang LY, Ji W, Tan LS (2007) Large concentration-dependent nonlinear optical responses of starburst diphenylaminofluorenocarbonyl methano (60) fullerene pentads. *J Mater Chem* 17:1826–1838
- Tsuboya N, Hamasaki R, Ito M, Mitsuishi M, Miyashita T, Yamamoto YJ (2003) Nonlinear optical properties of novel fullerene–ferrocene hybrid Molecules. *J Mater Chem* 13:511–513

28. Barbosa AGH, Nascimento MAC (2001) A new approach for designing molecules with large hyperpolarizabilities: substituted C<sub>36</sub> fullerenes as a test case. *Chem Phys Lett* 343:15–20
29. Tang GS, Chen XL, Zhang SY, Wang J (2004) The first trisaza-bridged (60) fullerene: Drilling a hole on the fullerene. *Org Lett* 6:3925–3928
30. Pichierri F (2005) Computer-aided design of nanostructured materials containing trisaza-bridged (60) fullerene. *Physica E* 29:689–692
31. Kurtz HA, Stewart JJP, Dieter KM (1990) Calculation of the nonlinear optical properties of molecules. *J Comput Chem* 11:82–87
32. Norman P, Bishop DM, Jensen HJA, Oddershede J (2005) Nonlinear response theory with relaxation: The first-order hyperpolarizability. *J Chem Phys* 123:194103–194118
33. Frisch MJ, Trucks GW, Schlegel HB, Scuseria GE, Robb MA, Cheeseman JR, Scalmani G, Barone V, Mennucci B, Petersson GA, Nakatsuji H, Caricato M, Li X, Hratchian HP, Izmaylov AF, Bloino J, Zheng G, Sonnenberg JL, Hada M, Ehara M, Toyota K, Fukuda R, Hasegawa J, Ishida M, Nakajima T, Honda Y, Kitao O, Nakai H, Vreven T, Montgomery JA, Peralta JE, Ogliaro F, Bearpark M, Heyd JJ, Brothers E, Kudin KN, Staroverov VN, Kobayashi R, Normand J, Raghavachari K, Rendell A, Burant JC, Iyengar SS, Tomasi J, Cossi M, Rega N, Millam JM, Klene M, Knox JE, Cross JB, Bakken V, Adamo C, Jaramillo J, Gomperts R, Stratmann RE, Yazyev O, Austin AJ, Cammi R, Pomelli C, Ochterski JW, Martin RL, Morokuma K, Zakrzewski VG, Voth GA, Salvador P, Dannenberg JJ, Dapprich S, Daniels AD, Farkas O, Foresman JB, Ortiz JV, Cioslowski J, Fox DJ (2009) Gaussian 09, Revision A.02. Gaussian Inc., Wallingford, CT
34. Wang FF, Li ZR, Wu D, Wang BQ, Li Y, Li ZJ, Chen W, Yu GT, Gu FL, Aoki Y (2008) Structure and considerable static first hyperpolarizabilities: new organic alkalides (M<sup>+</sup>@n<sup>6</sup>adz) M<sup>-</sup>(M, M'=Li, Na, K; n=2, 3) with cation inside and anion outside of the cage complexants. *J Phys Chem B* 112:1090–1094
35. Li Y, Li ZR, Wu D, Li RY, Hao XY, Sun CC (2004) An ab initio prediction of the extraordinary static first hyperpolarizability for the electron-solvated cluster (FH)2{e}(HF). *J Phys Chem B* 108:3145–3148
36. Lu T, Shao P, Mathew I, Sand A, Sun W (2008) Synthesis and photophysics of benzotexaphyrin: A near-infrared emitter and photosensitizer. *J Am Chem Soc* 130:15782–15783
37. Salzner U (2008) Investigation of charge carriers in doped thiophene oligomers through theoretical modeling of their UV/Vis spectra. *J Phys Chem A* 112:5458–5466
38. Qudar JL, Chemla DS (1977) Hyperpolarizabilities of the nitro-anilines and their relations to the excited state dipole moment. *J Chem Phys* 66:2664–2668
39. Marder SR, Beratan DN, Cheng LT (1991) Approaches for optimizing the first electronic hyperpolarizability of conjugated organic molecules. *Science* 252:103–106
40. Abe J, Nemoto Shirai Y, Nemoto N, Miyata F, Nagase Y (1997) Heterocyclic pyridinium betaines, A new class of second-order nonlinear optical materials: combined theoretical and experimental investigation of first-order hyperpolarizability through ab initio, INDO/S, and hyper-rayleigh scattering. *J Phys Chem B* 101:1910–1915
41. Nandi PK, Panja N, Ghanty TK (2008) Heterocycle-based isomeric chromophores with substantially varying NLO properties: A new structure-property correlation study. *J Phys Chem A* 112:4844–4852
42. Pan H, Gao X, Zhang Y, Prasad PN, Reinhardt B, Kannan R (1995) A new class of heterocyclic compounds for nonlinear optics. *Chem Mater* 7:816–821
43. Bera TK, Jang JI, Ketterson JB, Kanatzidis MG (2009) Strong second harmonic generation from the tantalum thioarsenates A<sub>3</sub>Ta<sub>2</sub>AsS<sub>11</sub> (A=K and Rb). *J Am Chem Soc* 131:75–77
44. Banerjee S, Mallikas CD, Jang JI, Ketterson JB, Kanatzidis MG (2008) <sup>1/∞</sup>[ZrPSe<sub>6</sub>-]: A soluble photoluminescent inorganic polymer and strong second harmonic generation response of its alkali salts. *J Am Chem Soc* 130:12270–12272